Real-time optical subtraction of photographic imagery for difference detection

John F. Ebersole and James C. Wyant

Interferometric techniques described in this paper permit real-time optical image subtraction of two input photograph transparencies without the necessity of intermediate processing steps (e.g., holograms or contact-print transparencies). These interferometric techniques allow the use of a white-light source as well as an extended light source, small input-collimator optics, and optical components with minimal requirements on wavefront quality. Experimental results with NASA LANDSAT (formerly ERTS) photographs are presented.

Introduction

This paper describes new techniques for real-time optical subtraction of photographic imagery.[1] The primary goal of this work was the development of a difference detection capability. There are many applications for such a technology, including earth resource studies, meteorology, automatic surveillance and/or inspection, pattern recognition, urban growth studies, and bandwidth compression. In general, there are several methods for obtaining optical image subtraction. Among them are interferometric and holographic methods, coding methods, and positive–negative superposition methods. A review of these techniques is given elsewhere.[2] The techniques described in this paper are interferometric.

Triangular Interferometer Method

Figure 1 shows one technique used for real-time optical subtraction of photographic imagery for difference detection. A triangular interferometer (comprised of two mirrors and a beam splitter) is used to superimpose the beams illuminating the photographic transparencies P_1 and P_2. The three output beams (actually four, with two superimposed) imaged by the output optics are shown in Fig. 1. If the amplitude transmittances of P_1 and P_2 are $t_1(x,y)$ and $t_2(x,y)$, respectively, the output I_3 is

$$I_3 = C\{t_1^2 + t_2^2 - 2t_1t_2 \cos[(2\pi/\lambda)\mathrm{OPD}]\}, \tag{1}$$

where C is a proportionality constant and where OPD is any optical path difference between the two beams carrying the P_1 and P_2 information. This equation assumes that the beam splitter equally divides the beam. The minus sign in front of the third term in Eq. (1) is due to an additional net phase change of π radians suffered by the P_2 beam (with respect to the P_1 beam) as a result of reflection from the beam splitter. When OPD $= m\lambda$ (m an integer), destructive interference occurs, and Eq. (1) can be written as

$$I_3 = C|t_1 - t_2|^2, \tag{2}$$

where any possible phase variations caused by the transparencies P_1 and P_2 are eliminated by using a liquid gate holder. If P_1 and P_2 are exactly superimposed (i.e., exact image registration is achieved), image subtraction will occur. [Image addition can be achieved if OPD $= (2m + 1)\lambda/2$.]

A triangular interferometer can produce shear, i.e., move one beam parallel to another, by displacements or rotations of the mirrors or beam splitter.[3] Thus, lateral superposition (i.e., x superposition) of P_1 and P_2 can be achieved in two ways: (a) by translating mirror 1 (or, equivalently, by translating mirror 2) or (b) by rotating mirror 1 (or mirror 2) about the y axis by an appropriate amount, say θ. Vertical superposition (i.e., y superposition) can be achieved by tipping one mirror through an appropriate amount, say ϕ, about an axis perpendicular to the axis of rotation for θ. (Lateral and vertical superposition can also be achieved using the beam splitter, but in our experiments it was more convenient to move one of the mirrors.) Rotation of a mirror will produce a change in the OPD. Thus the adjustment θ can serve a dual function—superposition and subtraction. The only other adjustment required is angular registration, say ψ adjustment, of the photographs back at the $P_1 - P_2$ photograph plane and perhaps tilt adjustment so

Both authors were with Itek Corporation, Optical Systems Division, Lexington, Massachusetts 02173 when this work was done. J. F. Ebersole is now with Aerodyne Research, Inc., Applied Sciences Division, Bedford, Massachusetts 01730. J. C. Wyant is now with the University of Arizona, Optical Sciences Center, Tucson, Arizona 85721.

Received 14 May 1975.

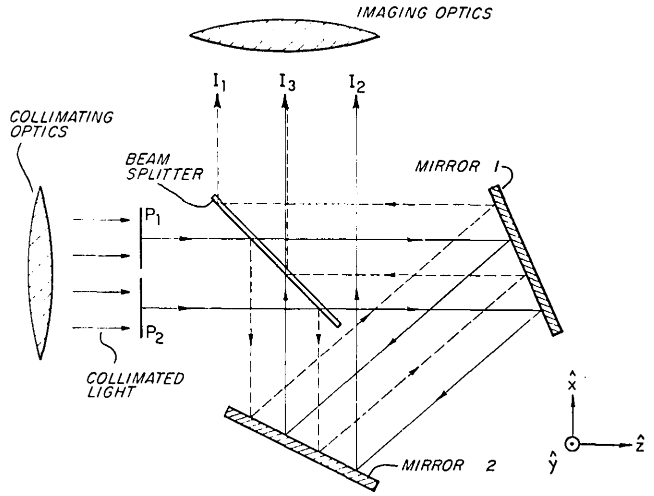

Fig. 1. Triangular interferometer to achieve, in real time, superposition and subtraction of two photographic transparencies (P_1 and P_2) and capable of using broadband or monochromatic as well as incoherent or coherent light sources. The outputs I_1 and I_2 correspond, respectively, to P_1 and P_2; the difference between P_1 and P_2 is present in I_3.

that P_1 and P_2 are in line with each other and are not tilted with respect to the incident collimated light. The superpositioning using z (or θ) and ϕ as well as the subtracting using θ are *real-time procedures.* The operator views the output I_3 while varying z, ϕ, and θ (and perhaps ψ and tilt) until registration and subtraction occur.

In order to obtain useful results from the subtraction of P_1 and P_2, it is necessary that P_1 and P_2 be simultaneously in focus at the output plane. As long as the mirrors and beam splitter are set so that the angle of incidence on both mirrors is the same for both beams, the optical pathlengths for both P_1 and P_2 will be equal. If one mirror is slightly misaligned by some amount $\Delta\theta$, the OPD introduced is only on the order of $X_P\Delta\theta$, where X_P is the width of each transparency. Experimentally, it is convenient to choose the angles of incidence on the beam splitter and each mirror to be 45° and 22.5°, respectively. It is then fairly straightforward, using retroreflection techniques, to align the system very accurately so that any residual OPD will be very small or, at the very least, smaller than the depth of focus of the output imaging lens. Having performed this initial alignment, an operator can then increment the rotation so that OPD = $m\lambda$ in order to achieve subtraction.

There is another real-time capability that can be added to the system. By inserting an appropriate neutral density filter (which may be N.D. = 0.0) in front of either P_1 or P_2, the average density levels of the two photographs can be matched or equalized. In this way it is possible to compensate for different sun illumination levels or different photographic processing of the two transparencies, thus eliminating a large amount of spurious noise caused by real differences between the photographs, but not caused by differences between the actual scenes.

If desired, a hard-copy output photograph can be taken of I_3 (and of I_1 and I_2, which also appear in the output plane). Since differences between P_1 and P_2 appear bright in I_3 to an observer, in a short-exposure (positive) photograph of I_3, the areas of P_1 and P_2 that are identical (i.e., that have no differences) will be almost completely dark, the partially similar areas will appear as various shades of gray, and the very different areas will appear brightest. If instead a photograph is taken with a longer exposure, the identical portions will then be faintly present, assisting the observer in determining the actual location of any changes (which appear even brighter) with respect to the constant background. In other words, use of variable-exposure photographic hard-copy output provides a capability for variable density level slicing.

Returning now to Eq. (2), the expression for I_3 can also be written as

$$I_3 = C\,|(I_1)^{1/2} - (I_2)^{1/2}|^2, \tag{3}$$

assuming $I_1 = t_1^2$ and $I_2 = t_2^2$. For applications where simply the *existence* of the differences (due, for instance, to temporal changes or to differences between multispectral data) is to be detected, the output I_3 described by Eqs. (1)–(3) will indeed provide positive evidence of changes. [In the experimental results, the Itek difference photograph and the LANDSAT imagery difference photographs are representative of Eqs. (1)–(3).] In some applications it is desired to know the difference $I_3 = C|I_1 - I_2|$ in addition to confirmation of the existence of any

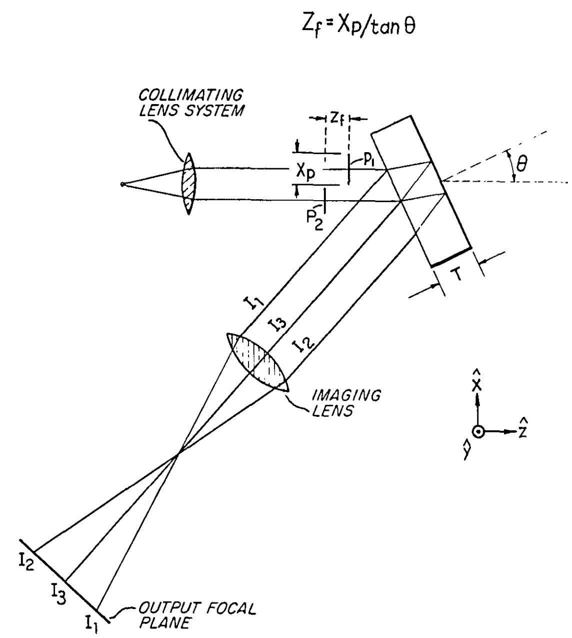

Fig. 2. Single shear plate interferometer for real-time superposition and subtraction of two photographic transparencies for use with monochromatic coherent light sources only.

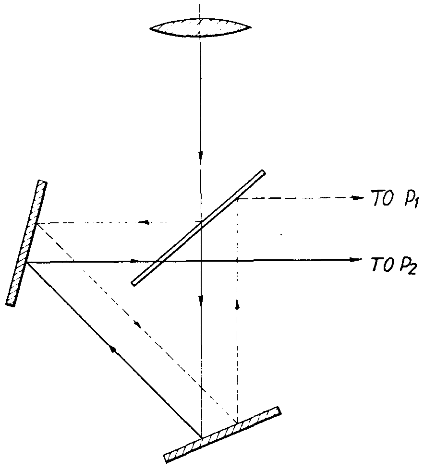

Fig. 3. Triangular interferometer to serve as a replacement for the collimating optics in Fig. 1, permitting use of smaller input collimater optics with less strict wavefront requirements as well as use of an extended light source.

change. It is possible to achieve this result by means of intermediate steps; however, real-time operation is thereby precluded. One procedure is to record individually P_1 and P_2 onto another transparency and then make a contact print of each such that after both steps the net film gamma of the transfer process is -2. (These might be combined by recording directly onto positive film with a gamma of -2.) When these new transparencies are subtracted, the output is $I_3 = C|t_1^2 - t_2^2|^2$ instead of Eq. (2). By recording this I_3 on film with a gamma of $-\frac{1}{2}$, the result is $I_3 = C|t_1^2 - t_2^2|$ or $I_3 = C|I_1 - I_2|$.

Plane-Parallel Plate Interferometer Method

Real-time optical subtraction of photographic imagery can also be accomplished by using a plane-parallel plate of glass instead of a triangular interferometer, as shown in Fig. 2. This method is simpler (in terms of the number of optical components), but requires some additional considerations. The beam illuminating P_1 travels through the shear plate, whereas the beam illuminating P_2 does not. Thus some astigmatism and spherical aberration will be introduced into the P_1 beam. The astigmatism can be compensated[4] by placing in the P_1 beam either (a) another plate of equal thickness T tipped by an equal amount but about an axis 90° to the first plate or (b) a wedged plate with the proper wedge angle. However, any spherical aberration from the first plate will be increased by the addition of a second plate. Another consideration involves the focusing of P_1 and P_2 at the same output image plane by the imaging lens. In order for P_1 and P_2 to be at the same conjugate distance from the lens, P_1 must be moved closer to the lens by some amount Z_f. From a simple geometric argument, the required value of Z_f is $X_P/\tan\theta$ (or $2X_P/\tan\theta$ if an astigmatism compensating plate described above is used). When $\theta = 45°$, at which the shear is approximately a maximum, $Z_f = X_P$ (or $2X_P$). If, for instance, it is desired to place P_1 and P_2 in the same liquid gate (and thus in the same plane), it would then be necessary to insert in the P_2 beam a separate plate to compensate for focus. This plate (of index n) would be set at $\theta = 0°$ (normal incidence); from geometrical arguments it can be shown that this plate would require a thickness $T = X_P n/(n - 1)\tan\theta$ [or $2X_P n/(n - 1)\tan\theta$] so that the P_2 path is foreshortened an appropriate amount. Although this would increase spherical aberration for the P_2 photograph, it would tend to balance out some of the spherical aberration in the P_1 beam.

It should be mentioned that the beam splitter in the triangular interferometer of Fig. 1 does introduce some astigmatism, as does a shear plate. However, the shear plate thickness must be sufficiently large that P_1 and P_2 can be superimposed, i.e., T must be large enough to produce a sufficient amount of shear. As an example, for $\theta = 45°$ and a glass plate of index $n = 1.5$, T must be greater than approximately $1.3X_P$, which can be a problem with large photographs. (However, an auxiliary lens system might be used to demagnify in real time the images of the photographs before they are subtracted.) On the other hand, the beam splitter in the triangular interferometer can be as thin as physically feasible, limited only by the mechanical strength necessary to hold a high-quality optical figure. This results from the fact that the shear, and thus the superpositioning, depend only on the separation and angular orientation of the two mirrors with respect to the beam splitter. In addition, the beam splitter makes an equal contributor to the optical paths of the P_1 and P_2 beams, so by correcting whatever astigmatism there is for one beam, the astigmatism in the other beam can be corrected at the same time.

Modifications

There is a modification to Fig. 1 that greatly improves the operation of the triangular interferometer technique. Figure 3 shows another triangular interferometer for use as the input optics in place of the collimating optics in Fig. 1. Since the effect of the two triangular interferometers is to shear the input beam (shown at the top of Fig. 3) and then superimpose again, the output pattern I_3 is the result of the interference of two nearly identical beams (excluding

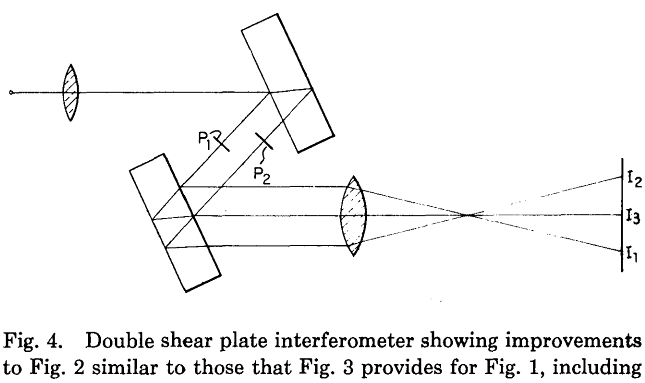

Fig. 4. Double shear plate interferometer showing improvements to Fig. 2 similar to those that Fig. 3 provides for Fig. 1, including the use of a broadband extended light source.

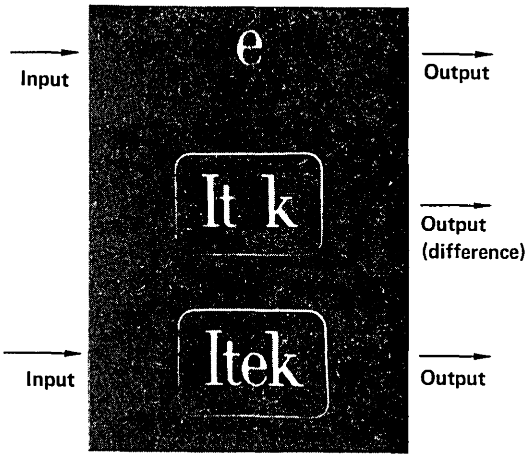

Fig. 5. Results of real-time optical image subtraction of two photographic transparencies (the letter e and the name Itek) using a single plane-parallel-plate interferometer.

the effect of P_1 and P_2). Hence, even relatively low-quality input collimating optics should be acceptable since the input wavefront deviations will be common to both interfering beams and will thus cancel when the two beams are superimposed. This reduces the over all requirements on the optical quality of the mirrors and beam splitters as well. In addition, the diameter of the collimator lens in Fig. 3 need only be as large as one photograph transparency, since the input beam is sheared by the first triangular interferometer into two beams, one for each photograph. This translates directly into size, weight, ease of fabrication, and thus cost savings. Finally, the introduction of another triangular interferometer permits the use of an extended light source as well as an incoherent white light source. [With one triangular interferometer, a white light source, but not an extended source, can be used for subtraction, because, after the geometrical paths for the P_1 and P_2 beams are made equal, there is a broadband π-radian phase shift introduced in the P_2 beam upon reflection from the beam splitter, as indicated in Eq. (1).] In practice it may be desirable to use a broadband spectral filter in conjunction with the white light source. The primary advantage of using an incoherent source is the elimination of speckle noise and extraneous interference effects that often accompany laser illumination. The primary advantage of an extended source is greater intensity in the input illumination to the system.

Figure 4 is a modification of Fig. 2 and provides advantages similar to those that Fig. 3 contributes to Fig. 1, i.e., smaller input collimator optics with less strict wavefront requirements as well as use of an extended light source. An incoherent white light source can also be used if the back surface of one plate is coated with a film of refractive index higher than the plate, thus causing P_1 (or P_2, depending on which plate is coated) to sustain an additional broadband π-radian phase shift. (In fact, with no compensating plates, the setup in Fig. 2 can use neither an incoherent nor an extended source because the OPD can never be made zero.)

Experimental Results

Figure 5 shows results of optical image subtraction using a single plane-parallel-plate lateral shearing interferometer. The two input photographic transparencies are the letter *e* and the name Itek shown at the top and bottom. The subtraction of the e from Itek is shown in the middle. A He–Ne laser (λ = 0.6328 μm) was used as the light source.

Figure 6 shows the three output photographs from a triangular interferometer: $I_1 = P_1$, $I_2 = P_2$, and the difference photograph I_3. P_1 and P_2 are NASA LANDSAT (formerly ERTS–Earth Resources Technology Satellite) photographs [band 6 (0.7–0.8-μm wavelength range)] taken at two different times. In

I_1 (P_1)
(October 21, 1972)

I_3 (difference)

I_2 (P_2)
(November 26, 1972)

Fig. 6. Results of optical image subtraction (center) of NASA LANDSAT (formerly ERTS—Earth Resources Technology Satellite) photographs using a triangular interferometer, but before compensation of the different average density levels of the transparencies. The accompanying text presents a more detailed description of the results.

I_1 (P_1)
(October 21, 1972)

I_3 (difference)

I_2 (P_2)
(November 26, 1972)

Fig. 7. Results of optical image subtraction (center) of the same NASA LANDSAT photographs in Fig. 6, but after real-time compensation (during the subtraction process) of the different average density levels of the transparencies. The accompanying text presents a more detailed description of the results.

I_3, differences show as various shades of gray—the greater the difference, the lighter it appears. The dark regions in I_3 are areas that exhibit no changes. In the lower left-hand corner of the I_3 photograph, less than pure white is evident. This is due to extraneous interference effects resulting from the coherence of the He–Ne laser light used in the breadboard system. For a brassboard system, an extended mercury light source or an extended white light source with a broadband spectral filter could be used, and these effects would then not be anywhere near as significant. New ice and snowfall in P_2 but not present in P_1 are especially evident in the upper left-hand corner of I_3. The crosses in P_1 and P_2 were added simply to aid in registration of the photographs with the breadboard processor; it may be noted that they are optically subtracted out of the I_3 photograph. Finally, although perhaps not so obvious in these reproductions, the average density level of P_1 is greater than that of P_2. As a result, although photograph I_3 shows the true differences between the P_1 and P_2 *photographs,* it is not representative of the differences between the corresponding irradiances of the P_1 and P_2 *scenes.* This is especially evident in the lower right-hand corner of I_3, where P_1 and P_2 photograph differences are evident, but where in reality no scene differences have taken place. This situation is shown corrected in Fig. 7.

In Fig. 7 are the same P_1 and P_2 photographs as in Fig. 6, only now the I_3 photograph is a much better representation of actual *scene differences* between P_1 and P_2. This is due to an approximate equalization, using a neutral density filter, of the average density levels of P_1 and P_2 as determined visually. As a result, it may be noted that the lower right-hand corner of I_3 is now almost completely black. At the same time, the real scene differences are enhanced or at the very least are much more obvious, e.g., the ice and snowfall changes in the upper left-hand corner of I_3. Also, small area changes become more obvious as well, due to an improvement in the SNR. It might be pointed out that there is considerable reduction of interference noise (due to the use of laser beam illumination) in the lower left-hand corner; as mentioned previously, this noise would be nonexistent with a mercury or a white light source.

Summary

The methods described above, as evidenced by the experimental results presented in Figs. 5–7, provide new capabilities for real-time detection of both the existence and location of differences between photographs. A partial listing of some advantages of the techniques include the following:

real-time subtraction of photographic imagery;

true subtraction (not multiplication) of optical transmittances;

parallel optical processor;

no serial scanning;

no computer required;

fast;

uses original photographic transparencies;

no intermediate photographic processing steps (e.g., hologram or contact-print transparency);

registration and subtraction adjusted simultaneously;

compensates for different average density levels of transparencies (caused by different sun illumination or by different photographic processing);

visual or photographic hard-copy output;

use of an incoherent light source (triangular interferometer only).

For the modified versions (the use of an additional triangular interferometer or another shear plate), the additional capabilities include for both methods

use of an incoherent light source,

use of an extended light source,

small input optics (collimator diameter need not exceed width of one transparency),

processor technique greatly reduces required wavefront quality of system optical components.

The authors thank V. Bennett, L. Seppala, and B. Willard of Itek Corporation for their helpful discussions and comments. A special note of thanks is extended to J. C. Barnes, Manager of Earth Resource Studies at Environmental Research & Technology, Inc. (Lexington, Mass.), who supplied the NASA LANDSAT photographs.

References

1. J. F. Ebersole and J. C. Wyant, J. Opt. Soc. Am. 64, 1402A (1974).
2. J. F. Ebersole, Opt. Eng. 14, 436 (1975).
3. W. H. Steel, *Interferometry* (Cambridge U.P., London, 1967), pp. 94–95.
4. J. McLaughlin, "Properties of Plane Parallel Plates in Convergent Light," M.E.E. thesis (Dept. of Electrical Engineering, Northeastern University, 1972), pp. 33–46.